Modeling the Human Body/Seat System in a Vibration Environment

Jacob Rosen[1]
Department of Electrical Engineering,
Box 352500,
University of Washington,
Seattle, WA 98195-2500

Mircea Arcan*
Department of Biomedical Engineering,
Department of Solid Mechanics,
Materials and Structures,
Faculty of Engineering, Tel-Aviv University,
Ramat-Aviv, 69978, Tel-Aviv, Israel

The vibration environment is a common man-made artificial surrounding with which humans have a limited tolerance to cope due to their body dynamics. This research studied the dynamic characteristics of a seated human body/seat system in a vibration environment. The main result is a multi degrees of freedom lumped parameter model that synthesizes two basic dynamics: (i) global human dynamics, the apparent mass phenomenon, including a systematic set of the model parameters for simulating various conditions like body posture, backrest, footrest, muscle tension, and vibration directions, and (ii) the local human dynamics, represented by the human pelvis/vibrating seat contact, using a cushioning interface. The model and its selected parameters successfully described the main effects of the apparent mass phenomenon compared to experimental data documented in the literature. The model provided an analytical tool for human body dynamics research. It also enabled a primary tool for seat and cushioning design. The model was further used to develop design guidelines for a composite cushion using the principle of quasi-uniform body/seat contact force distribution. In terms of evenly distributing the contact forces, the best result for the different materials and cushion geometries simulated in the current study was achieved using a two layer shaped geometry cushion built from three materials. Combining the geometry and the mechanical characteristics of a structure under large deformation into a lumped parameter model enables successful analysis of the human/seat interface system and provides practical results for body protection in dynamic environment. [DOI: 10.1115/1.1559894]

Keywords: Human-Body Vibration, Apparent Mass, Sitting Posture, Chair, Seat, Contact, Cushion, Lumped Parameter Model

1 Introduction

Man-made artificial environments have exposed the human body to more extreme conditions than those of the natural environment. The human body tolerance in vibration environments may limit the ability of the human to operator high performance vehicles and in that way to limit the overall performance of the entire system [1,2]. Moreover, prolonged or frequent exposure to dynamic environments may cause general physical and physiological disorders or tissue degeneration [3]. Thus, special aspects have to be considered in order to protect the human body. The basic analytical tool for developing protective devices is a model simulating the human body in a sitting posture exposed to vibration environments. This model should include two subsystems that represent the human body dynamics and the seat/cushion. In studying and developing any type of protection in a vibration environment it is vital to consider both the human body dynamics and its interfaces with the environments.

Both experimental and analytical approaches were used to study human body dynamics in a vibration environment. However, most of the models focused on studying human body dynamics only along the vertical axis with respect to the ground [4–7]. A systematic experimental work performed by Fairley and Griffin [8,9] studied the apparent mass frequency response function of a seated human body given different body postures, environmental effects, vibration axes, and vibration magnitudes. Although this study provided profound experimental data about the human body's apparent mass the multi degrees of freedom (DOF) lumped parameter model associated with that database, as with many other models, represented the human body in a single sitting posture exposed to vertical vibration.

Interfaces of the human body with supporting surfaces (e.g., body/cushion-seat, residual limb/prosthetic socket) present an important design challenge in terms for providing adequate mechanical support in static and dynamic conditions in addition to protecting soft tissue from trauma and ulceration [7]. Several experimental devices have been developed to measure the contact stress distribution of the human body/seat interface in both static and dynamic conditions e.g. for flexible/rigid bodies (static) - the Contact Pressure Display (CPD) [10,11], the Electronic Shape Sensor (ESS)/Computer Aided Seating System (CASS) [12] and for flexible/flexible bodies (dynamic)-the Contact Geometry Modular Resistive Transducer (CGMR) [13].

Optimizing a custom-made cushion is ongoing research mainly focused on static conditions. Cushion design was aimed at providing loading conditions characterized by low peak and gradient interface pressures. Custom contour foam cushions with various densities lowered the interface pressure compares to flat foam cushions [14]. A shape-based two-phase custom cushion design protocol was proposed by Brienza et al. [15]. The method of choice for modeling this interface in static conditions only is Finite Element Analysis (FEA) [16,17]. However, the nonlinear viscoelastic nature of soft tissue, in addition to the large deformation involved during the loading process, are still challenging this technique. The lack of a numerical model that describes seated human body dynamics for different sitting postures, vibration axes, and environmental effects has caused seat/cushion design to be based on experimental techniques. Moreover, previous studies [14,15] modified either the shape or the material composites with different optimization criteria only in static conditions. Since the nature of

[1]Corresponding Author Dr. Jacob Rosen, Department of Electrical Engineering, Box 352500, University of Washington, Seattle WA 98195-2500, USA FAX: 206-543-3842 E-mail: rosen@u.washington.edu

*Deceased on June 15, 2000

Contributed by the Bioengineering Division for publication in the JOURNAL OF BIOMECHANICAL ENGINEERING. Manuscript received July 1999; revised manuscript received August 2002. Associate Editor: M. G. Pandy.

seat cushion design for vibration conditions is trial and error, the design procedure becomes complicated and requires extensive data analysis. Simulation, based on a numerical model can shorten and simplify the design procedure.

The objective of this study was to develop a lumped parameter model describing the apparent mass of a seated human body in all three main vibration directions (X,Y,Z). The global human body model was further developed to describe the local dynamics of the human pelvis/vibrating seat contact using a cushioning interface. Studying this unique interface with the model led to the development of basic guidelines for composite cushion design that incorporated both the shape and materials composition for human body protection in vibration environments.

2 Method

The multi DOF lumped parameter model of a human body in a sitting posture was developed as two subsystems. The first subsystem represented the apparent mass phenomenon as the global human dynamics. The model for the vertical direction (Z) was originally proposed by Fairley and Griffin [14]. This model was further generalized, in this study to the three vibration axes (X,Y,Z) simulating the effects of various sitting postures and environmental characteristics on the apparent mass phenomenon. The second subsystem represented the local dynamics of the human pelvis/vibrating seat contact with a cushioning interface. The two dimensional lumped parameter model of the human pelvic structure coming in contact with the vibrating seat was then added to the global human body subsystem model. The combined model represented the two substructures (human pelvis and cushion) both geometrically and mechanically and focused on describing the vertical contact forces generated at their interface. The following subsections include a detailed description of each subsystem.

2.1 Global Dynamics-Apparent Mass. The human body exhibits complex dynamic behavior when exposed to a vibration environment. Apparent mass is one of several biomechanical engineering characteristics (e.g., mechanical stiffness and mechanical impedance) defined for describing the human body's biomechanical frequency response when exposed to a vibration environment.

The apparent mass of a seated human body was represented by the complex transfer function (frequency dependent):

$$M(s)=\frac{F(s)}{A(s)} \tag{1}$$

where: $M(s)$ is the apparent mass; $F(s)$ is the force transmitted at the human body/seat interface, $A(s)$ is the acceleration of the seat, and s is a complex frequency variable ($s=j\omega$).

The linear lumped parameter model (Fig. 1) represented the apparent mass of the human body in several sitting body postures and environmental conditions in three vibration directions: vertical (Z), fore and aft (X), and side to side (Y). Using Fairley and Griffin's experimental protocol [8,9], the following seated body postures and environmental conditions were simulated by the model: (i) reference body posture, (ii) backrest, (iii) footrest, (iv) vibration magnitudes, (v) muscle contraction. The consistent experimental work of Fairley and Griffin offered the ideal baseline for a comparison between experimental data and the numerical model simulations developed in this study.

Each axis of the apparent mass was defined by a two DOF model and was independent of the other two orthogonal axes (Fig. 1). The masses used in the model were: m_1, representing upper body; m_3, representing the feet that were moved with respect to the seat plate; and m_2, representing the lower body which did not move at all with respect to the same plate. Similarly, the stiffness and damping coefficients (K_b, K_f, C_b, C_f) were, like the masses, related to specific directions (X, Y, Z). In cases where a footrest was used and moved with the seat plate, a redundant model version was used by setting the mass m_3 and the viscoelastic elements K_f C_f to zero, since there is no relative movement between the footrest and the seat plate. However, when feet were supported on a stationary footrest, the spring and damper (K_f, C_f) connecting the mass m_2 to the stationary footrest were not omitted due to relative movements between the footrest and the seat, influencing the overall dynamics.

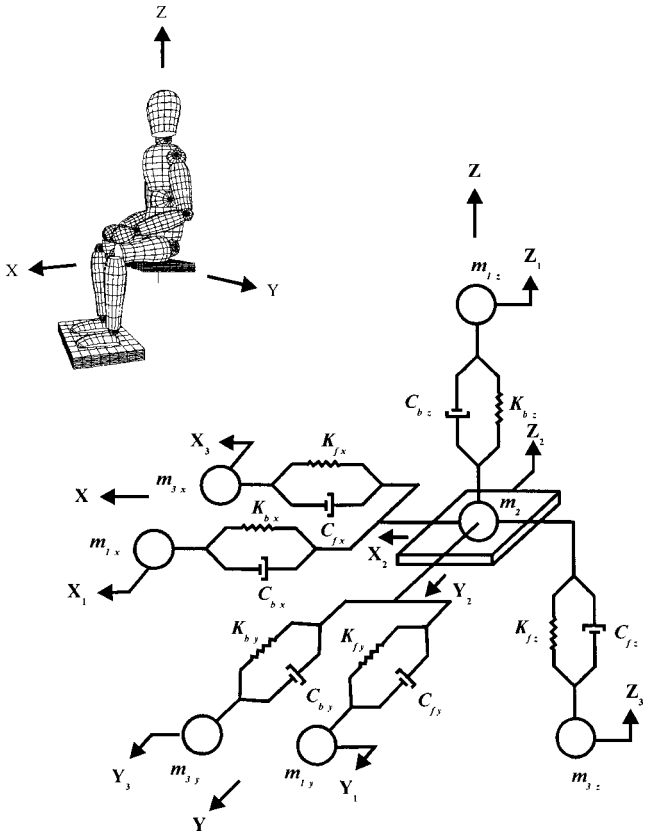

Fig. 1 Lumped parameter model of a seated human body with three separate vibration axes

To achieve the best representation of the experimental results using the numerical model, several basic guidelines had to be established for optimal selection of the model parameters. The lumped parameter models DOF (one or two) were selected based on the number of vibration modes appearing in the experimental data. The mass components of the model were considered to be non-variant parameters and defined by Fairley and Griffin [8,9], whereas the viscoelastic elements were defined as variant parameters. The numerical values of the stiffness coefficients (K_b, K_f) and damping coefficients (C_b, C_f) were evaluated for each model setup using optimization technique with bounded constraints on the parameters, setting them to have only positive values ($K_b, K_f, C_b, C_f > 0$). The initial values for the stiffness and damping coefficients were approximated based on the experimental damped resonance frequencies and the corresponding apparent mass modulus. The optimization cost function was defined as the root mean square of the difference between the experimental apparent mass data obtained by Fairley and Griffin [8,9] and the model prediction in the frequency spectra of 0.25–20 Hz with a resolution of 0.25 Hz. The final selected sets of the model parameters were those that minimized the cost function.

2.2 Local Dynamics - Human Body/Seat Contact. The contact between two deformable bodies is a three dimensional phenomena; however in a special case of the human body/seat interface, it can be simplified to be two dimensional one. A typical map of the contact force distribution generated between the human body in a seated posture and a stiff seat that was measured by

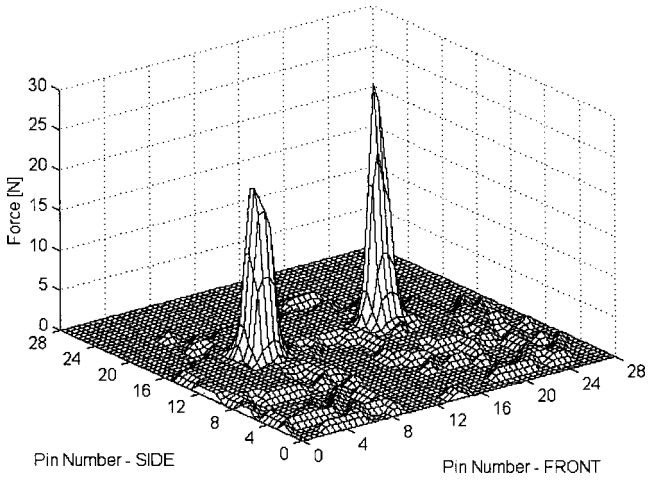

Fig. 2 Measured contact forces at the human/stiff seat plat interface (CPD) representing as a 3-D meshed plot of the sitting area (Pins distance along the plate side is 16 mm and along the plate front/back is 12 mm)

the CPD, is shown in Fig. 2. This map could be divided into two zones: (*i*) a low level zone which described the contact of the thighs, and (*ii*) two significant peak zones generated by the structure of the pelvis, namely, the Ischial Tuberosities. The *loaded strip* [12,18] is defined as the contact area, 48 mm wide which included the Ischial Tuberosities region, where the highest contact stress peaks are included, for representing the most significant signature of the entire sitting area. This loaded strip, averaged in the sagittal plane, was farther used by the model to simulate the contact area.

The non-linear, two-dimensional, multi degree of freedom lumped parameter model (Fig. 3) had two components: the human body, and the seat. The human body itself contained two subsystems. One subsystem simulated the global human dynamic response, known as the apparent mass effect. The apparent mass phenomenon was simulated by the lumped parameter model along the Z axis detailed in section 2.1. Note that m_2 and m_{1z} of the global human dynamics (apparent mass-Fig. 1) corresponded to m_{ls2} and m_{ls1} in the human/seat contact model (Fig. 3(*a*)), respectively. The second subsystem was half of the symmetric human pelvis above the loaded strip (Figure 3(*a*, *b*)). These two combined subsystems came in contact with the second module of the model representing the seat. Two seat options were examined: (*i*) a stiff seat plate (Fig. 3(*c*)) and (*ii*) a composite flexible cushion with different configurations (Fig. 3(*d–g*)).

Based on the viscoelastic nature of both soft tissues and cushion materials, the Voigt model (a spring in parallel to a damper) was selected to simulate the mechanical behavior of the materials at the interface [18,19]. Each column of Voigt model elements represented a contact area of 12 mm×16 mm. Those particular dimensions were selected based on the sensor size of the CPD instrument [10], which was one of the experimental systems used for the model evaluations. The unloaded contour of the soft tissue above the loaded strip was represented by *Ti*, the soft tissue thickness, and *Di*, the clearance between tissue and seat plate (Fig. 3(*b*)). These geometrical parameters were measured from a human pelvis cross-section obtained by X-ray imaging [11,16]. The masses of the cushion ($m_1, \ldots, m_{26}$) were represented in the model by lumped masses. In principle, 26 different viscoelastic

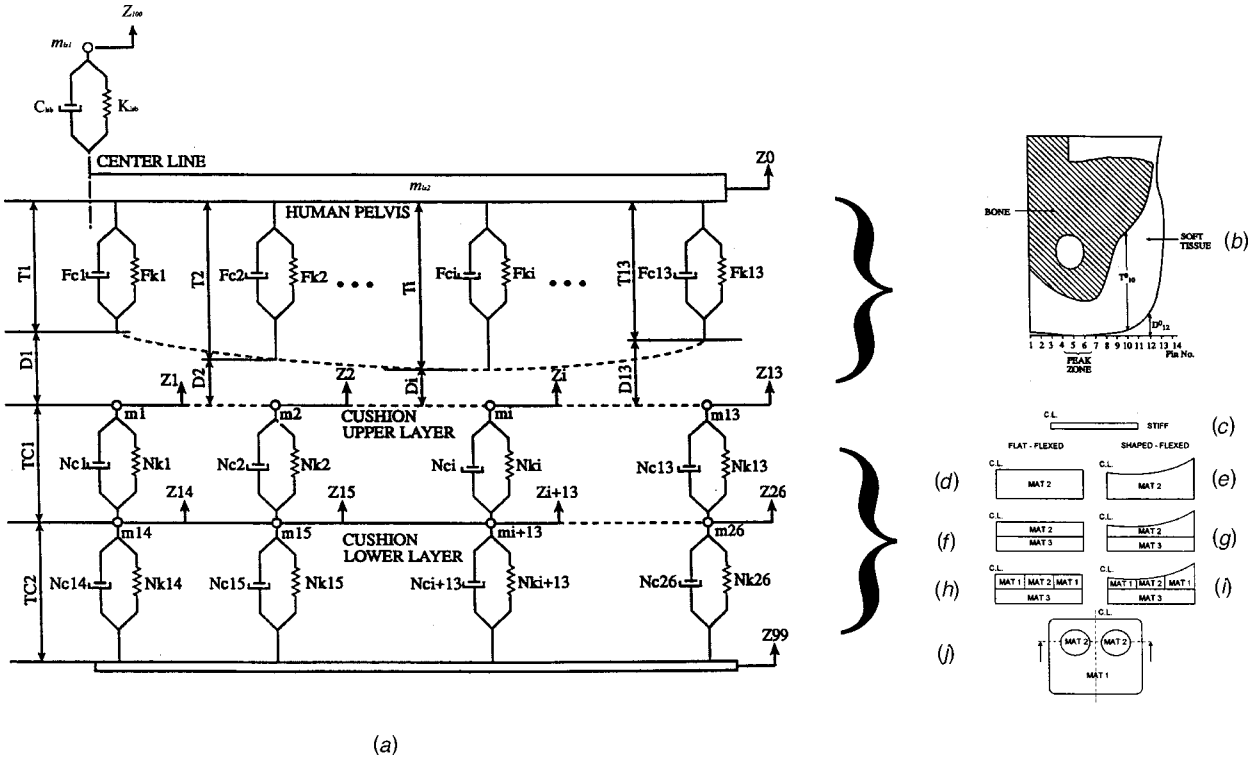

(*a*)

Fig. 3 The lumped parameter model of the human/seat contact with a two-layer composite cushion: (*a*) Lumped parameter model, (*b*) Schematic geometry description of a typical human pelvis and soft tissue cross-section above the loaded strip (Distance between pins-12 mm). Cushion configurations-schematic representation of half cross section (C.L.-Center Line): (*c*) Stiff seat, (*d*) Flat homogeneous cushion, (*e*) Shaped homogeneous cushion, (*f*) Flat, two-layer heterogeneous cushion (2 materials), (*g*) Shaped, two-layer heterogeneous cushion (2 materials), (*h*) Flat, two-layer heterogeneous cushion (3 materials), (*i*) Shaped, two-layer heterogeneous cushion (3 materials), (*j*) Top view of upper layer three-material cushion.

materials could be used for the two-layer cushion structure and simulated by the model. However, due to practical design considerations discussed in section 2.3, only three materials were selected for designing the cushion.

The viscoelastic forces applied by each Voigt model element representing the human body's soft tissue (F_{ki},F_{ci}) and the cushioning materials (N_{ki},N_{ci}), were composed from the viscoelastic elements and shape function defining the boundary conditions. The elastic force components (F_{ki} in Eq. 2), and the viscous force component (F_{ci} in Eq. 3) of the i'th soft tissue Voigt element were defined as follows:

For i=1, . . . ,13

$$F_{ki}=F_{0i}\left(\left[\frac{1}{1-\Delta z_i/T_i^0}\right]^r-1\right) \tag{2}$$

$$F_{ci}=c_i\Delta\dot{z}_i \tag{3}$$

where T_i^0 is the soft tissue thickness (unloaded) and F_{0i}, r, c_i are material constants.

The elastic force components (N_{ki} in Eq. 4) and the viscous force components (N_{ci} in Eq. 5) of the i'th Voigt elements representing the upper layer (i=1, . . . ,13) and the lower layer (i =14, . . . ,26) of the cushion with thickness of TC_{1i}, TC_{2i} respectively. The material properties functions $f_{mat(j)}$ of j's materials were defined as follows:

For i=1, . . . ,26

$$N_{ki}=f_{mat(j)}\left(\frac{\Delta z_i}{TC_i}\right) \tag{4}$$

$$N_{ci}=N_{0ci}\Delta\dot{z}_i \tag{5}$$

The shape and constraint functions defined as unit step functions multiplied each one of the Voigt elements. The main idea behind the shape and constraint functions was to use them as virtual switches that turn on or off the continuous solution of the motion equations according to the shape of the human body's soft tissue and the cushion's upper layer contour. The unit step function returned a unit value during the entire contact process between the soft tissue and the upper layer of the cushion. The zero value indicated that no contact existed. In addition as constraint functions they imposed the fact that the cushion materials could only be compressed and not stretched returning a unit value during a compression process and a zero value in elongation.

The viscoelastic characteristics of the Voigt model elements were based on indentation experiment measurements of the soft tissue at different locations along the loaded strip [16]. In addition, stress/strain experimental data of three commercial foam materials, obtained by utilizing a rectangular 12 mm×16 mm indentor moving at a strain rate of 37 mm/s, were further used for representing the Voigt elements of the cushioning (Fig. 3(*d*–*i*)).

To preserve the generality of the model, several parameters were defined as ratios. The partial mass of the human body above the loaded strip ($M_{ls1}+M_{ls2}$) was defined based on experimental measurement to be 60% of the total mass [11,16]. The mass ratio M_{ls1}/M_{ls2} was 7.6 [8]. For the viscoelastic parameters (K_{lsb},C_{lsb}) in Fig. 3(*a*), the damping ratio (ζ) and the natural resonance frequency (f_n) were selected as 0.475 and 5Hz, respectively [8]. The viscoelastic parameters of the soft tissue were selected as follows: F_{0i}=10 N (for i=1, . . . ,5,8, . . . ,13), F_{0i} =50 N (for i=6,7), C_i=50 Nsec/m (for i=1, . . . 13), and r =0.4 [11,16]. These parameters were selected by fitting Eqs. 2 and 3 to data obtained from the vertical soft tissue indentation experiment performed at various locations along the loaded strip. The viscoelastic parameters of the cushion materials were based on a specific selection of commercial cushioning materials. The mass of each cushion component in the model was correlated with a piece of material with a dimension of 12×16×L mm, where L was the local cushion thickness. The soft tissue parameters located at the loaded strip under the pelvis were defined based on a typical human pelvis/soft tissue geometry (T_i^0,D_i^0) in Fig. 3(*b*).

2.3 Cushion Design Goals. Two main design goals had to be achieved for the cushion to protect the human body in a vibration environment. The first goal was to create, as much as possible, a quasi-uniform distributed map of contact forces. In that way the cushion supports the human body weight, avoiding high local pressure zones which usually generated at the pelvic structure/seat interface. The second goal was to control the resonance frequency of the human body/seat system. By specifying the viscoelastic properties of the cushion's composite materials, the displacements, forces, and therefore the energy being transferred to the human body was attenuated at the human body resonance frequency. In that way the cushion was acting as a mechanical filter, absorbing part of the energy and protecting the human body from the external vibration environment [20].

Different types of cushion setups-in terms of geometry and material composition-were simulated and tested using the model (e.g., flat and shaped homogeneous cushions Fig. 3*d*, *e*, and flat and shaped heterogeneous cushions Fig. 3(*f*–*i*)). The shaped cushion geometry had an inverse duplication of the soft tissue contour in an unloaded condition. The top view of the upper layer of a cushion structured from three materials is depicted in Fig. 3(*j*). The motivation for using a two-layer shaped cushion composed of three materials was to provide sufficient degrees of freedom in terms of the design to achieve the design goals of overcoming the complex anatomy of the pelvic structure and high contact forces under the Ischial Tuberosities. The primary idea was to place the softest material of the three under the Ischial Tuberosities region, where high contact forces developed. The hardest material was placed on the rest of the top layer to support the reminder of the pelvic structure. The material with medium stiffness was used for the cushion's lower layer, creating a dual region reaction and preventing contact with the stiff seat plate underneath the cushion.

3 Results

3.1 Global Dynamics - Apparent Mass. The human body in the reference sitting posture presented two heavily damped resonance modes of vibration along the X and Y axes and a single resonance mode along the Z axis (Fig. 4(*a*)). The main effect of the backrest was along the X and Y axes where it reduced the number of resonance modes from two to one (Fig. 4(*b*)). Moreover, the resonance frequencies and apparent mass modulus with a backrest were higher than corresponding parameters of the first mode without the backrest. The minor effect on the apparent mass along the Z axis was displayed as a small decrease in the apparent mass modulus at the resonance frequency without any change to the resonance frequency itself. As indicated by the model parameter optimization process, the overall increase in upper body stiffness and damping when a backrest was used, was simulated by increasing the values of the viscoelastic coefficients (K_b,C_b) relative to the parameters of the sitting posture without a backrest (Table 1).

The greatest effect of footrest location in a sitting posture on the apparent mass was evidenced at low frequencies below the resonance frequency (Fig. 4(*c*)). At 1 Hz, when the footrest was located at its highest position, the apparent mass approximately equaled the static weight of the subject on the sitting platform. As the footrest moved to its lowest location the value of the apparent mass halved relative to the previous case. An inverse effect, however minor in its magnitude, was exhibited at frequencies above the resonance frequency. As a result of the model parameter optimization process, the major effect of stiffening the thighs, as the footrest was lowered, was simulated by increasing the values of the viscoelastic coefficients (K_f,C_f), which represent the lower legs in the model. When the footrest was removed completely, so that the feet hung freely, a general increase of the apparent mass

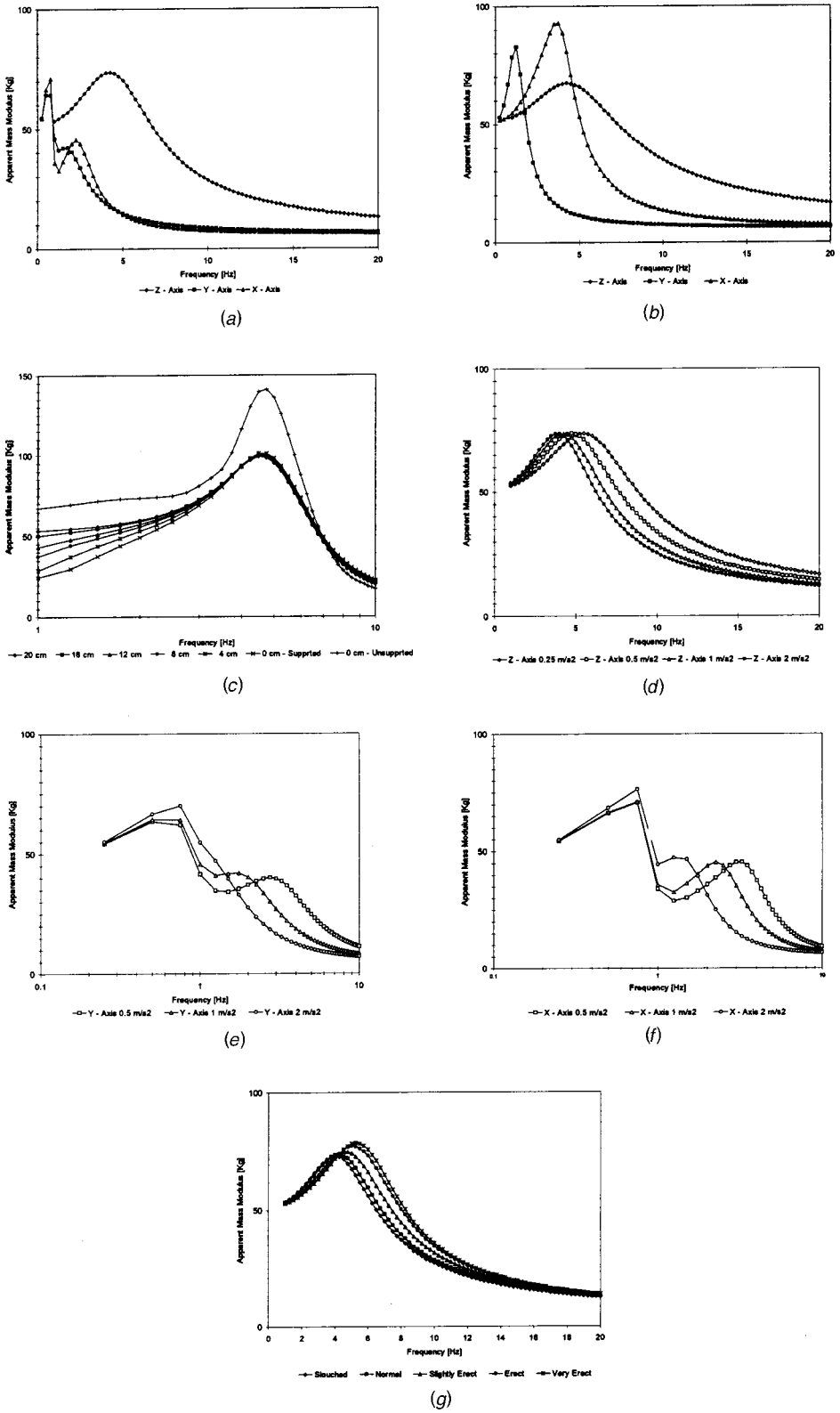

Fig. 4 Apparent mass modules in sitting posture-model simulation results (*a*) Sitting posture without a backrest (Reference posture) (*b*) Sitting posture with a backrest (*c*) Stationary footrest (*d*) Vibration magnitude-Z axis (*e*) Vibration magnitude-Y axis (*f*) Vibration magnitude-X axis (*g*) Muscle tension

Table 1 Apparent mass model parameters-m [Kg], K [N/m], and C [Ns/m].

Effect	Parameter	Axis	m_{1t}	m_2	m_{3i}	K_{bi}	C_{bi}	K_{fi}	C_{fi}
Reference	1 m/s^2	X	22.8	6.0	22.8	506.3	51.3	5625.6	508.5
	1 m/s^2	Y	22.8	6.0	22.8	506.3	75.2	3600.4	567.2
	1 m/s^2	Z	45.6	6.0	/	45005.3	1360	/	/
Backrest	1 m/s^2	X	22.8	6.0	22.8	11723.7	447.8	15606.2	516.6
	1 m/s^2	Y	45.6	6.0	/	3271.1	289.6	/	/
	1 m/s^2	Z	45.6	6.0	/	49789.4	1779.6	/	/
Footrest Height	0 Cm-(Unsupported)	Z	45.6	6.0	11.5	44947.0	506.0	2000.0	151.6
	0 cm (Touching)	Z	45.6	6.0	/	44947.0	800.0	2000.0	151.6
	4 cm	Z	45.6	6.0	/	44947.0	800.0	1285.0	121.5
	8 cm	Z	45.6	6.0	/	44947.0	800.0	752.0	92.9
	12 cm	Z	45.6	6.0	/	44947.0	800.0	472.0	73.6
	16 cm	Z	45.6	6.0	/	44947.0	800.0	150.0	41.5
	20 cm	Z	45.6	6.0	/	44947.0	800.0	0.0	0.0
Vibration Magnitude	0.5 m/s^2	X	22.8	6.0	22.8	506.0	51.0	11026.0	771.0
	2 m/s^2	X	22.8	6.0	22.8	506.0	51.0	2025.0	305.0
	0.5 m/s^2	Y	22.8	6.0	22.8	506.0	75.0	9507.0	89886.0
	2 m/s^2	Y	22.8	6.0	22.8	506.0	75.0	1406.0	13296.0
	0.25 m/s^2	Z	45.6	6.0	/	75521.0	1762.0	/	/
	0.5 m/s^2	Z	45.6	6.0	/	56959.0	1532.0	/	/
	2 m/s^2	Z	45.6	6.0	/	37894.0	1248.0	/	/
Muscle Tension	Slouched	Z	45.6	6.0	/	40960.0	1325.0	/	/
	Normal	Z	45.6	6.0	/	45005.0	1360.0	/	/
	Slightly Erect	Z	45.6	6.0	/	53470.0	1436.0	/	/
	Erect	Z	45.6	6.0	/	62665.0	1453.0	/	/
	Very Erect	Z	45.6	6.0	/	66328.0	1443.0	/	/

was seen in all the frequency spectra. This phenomenon was simulated by adding the mass of the feet (m_3) allowing it to move freely relative to the seat plate (Table 1).

The effect of the vibration magnitudes on the apparent mass of a seated human body was exhibited as an overall stiffness decrease of the system as vibration magnitudes increased. These phenomena were axes-dependent; however, they were manifested as a resonance frequency shift toward lower frequencies as vibration magnitudes increased (Fig 4(d–f)). The resonance frequency shift while maintaining the same modulus at that point was simulated by decreasing the model parameters K_f, C_f (X, Y axis) and K_b, C_b (Z axis) appropriately as the input vibration magnitude increased (Table 1). Although a linear model was used, the relationship between the input vibration magnitudes and the model parameters was nonlinear.

The level of muscle contraction adopted by the subjects determined the overall stiffness of the entire body. The resonance frequency and the apparent mass modulus increased as muscle contraction became more erect (Fig. 4(g)). For simulating this phenomenon the model parameter optimization process indicated that the elastic coefficient K_b had to be increased associated with decreasing the damping ratio of the upper body (Table 1).

3.2 Local Dynamics - Human Body/Seat Contact. Model simulation results and the experimental data obtained by using the CPD method in static conditions are depicted in Fig. 5. The static vertical contact force distribution at the interface between the soft tissue and the stiff plate under the loaded strip represented by the model simulation was in the range of upper and lower accuracy limits of the experimental measurements marked by the error bars. A high contact force zone noted by the peak was generated due to the pelvis anatomy and the thinner layer of soft tissue under the Ischial Tuberosities. A relatively thick layer of soft tissue produced evenly distributed contact forces at the rest of the interface area.

In dynamic conditions, the maximum vertical contact force distribution was plotted for different input vibration frequencies of the stiff plate (Fig. 6(a)). The peak zone of the contact force distribution, created by the Ischium bone, was notable for all input vibration frequencies. The peak zone in the frequency domain was at 4.25 Hz, indicating the resonance frequency of a seated human body along the vertical axis. For each point at the same lateral distance, the dynamic contact force at the resonance frequency was about 1.5 times greater then the static contact force. For frequencies above 8 Hz, the contact forces had lower values compared to the static conditions and further decreased as the input frequency increased.

The influence of cushion shapes and materials composition on contact force distribution at the human body/seat interface was studied using different cushion setups. Experimental stress-strain diagrams for three commercial foamy rubber-like materials se-

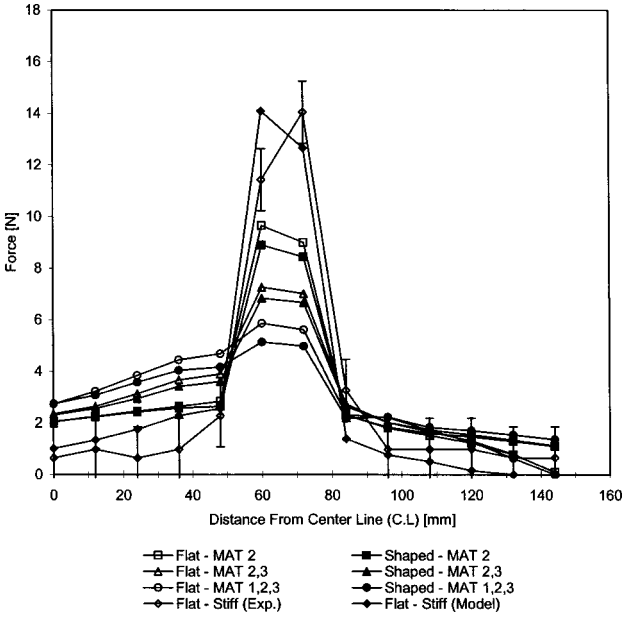

Fig. 5 Static contact force distribution of the loaded strip interfacing with a stiff and various configurations of flexible cushions as predicted by the model. The experimental data obtained by the C.P.D. are plotted for the stiff seat only. The error bars define the accuracy range of the experimental data.

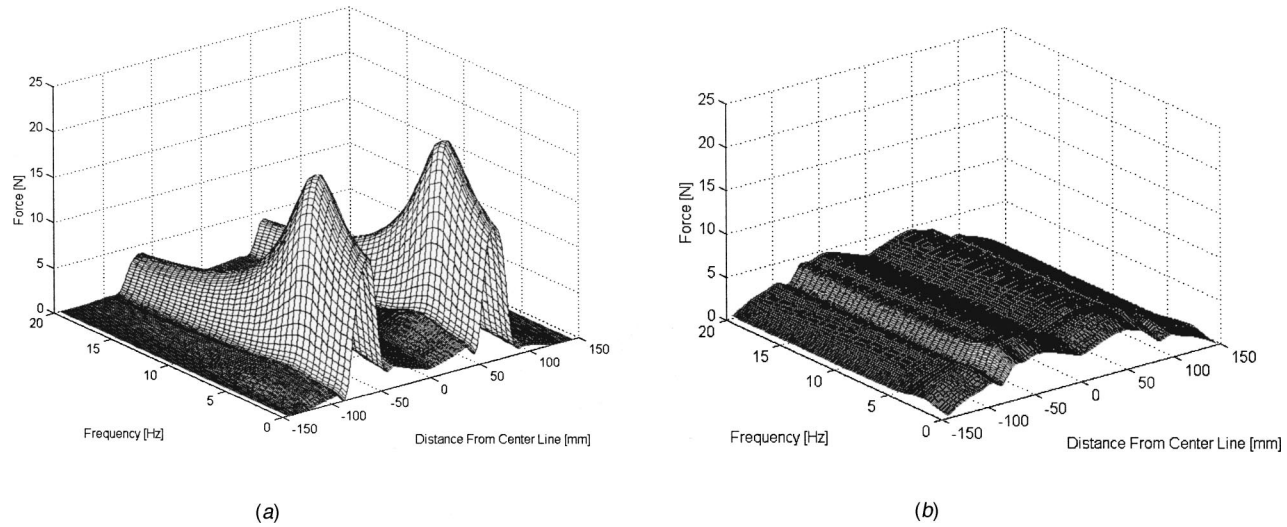

(*a*) (*b*)

Fig. 6 Dynamic vertical contact force distribution of the human pelvis (loaded strip) interacting with a stiff seat interface (*a*), and a composite, two-layer flexible shaped cushion (*b*)

lected to construct the cushion are plotted in Fig. 7. The maximum vertical contact force distributions generated while the human pelvis loaded strip was interacting with various cushion configurations are plotted in Fig. 5 (static conditions) and Fig. 6(*b*) (dynamic conditions for the cushion defined by Fig. 3(*i*)). The static contact force distribution was divided into three pairs of typical diagrams. Each pair represented the interaction with two cushions composed of the same materials but with a different structure, flat or shaped (Fig. 5). For each of these pairs, the vertical contact force distributed more evenly for the shaped cushion then for the flat one. Lower contact forces were applied on the soft tissue at the zone of about 120 mm from the center line in the lateral direction when a shaped cushion was used.

From the materials point of view, heterogeneous cushions could evenly distribute contact forces. The best result from the cushion configurations tested was achieved by a shaped, two-layer cushion composed of three materials (Fig. 3(*i*)). The cushion material under the Ischial Tuberosities, where the peak zones of the vertical contact forces appeared, needed the lowest stiffness out of the three materials (MAT2). The other zones of the cushion's upper layer were constructed from the material with the highest stiffness (MAT1). The cushion material (MAT3) with a stiffness value in between the upper layer materials (MAT1, MAT2) was used for the lower layer.

Comparing the dynamic vertical contact force distribution generated between the human body loaded strip interacted with two optional seats-a stiff seat plate (Fig. 6(*a*)) and a composite two layer cushion (Fig. 6(*b*)) indicated that for any given input frequency in the range of 0–20 Hz, the contact forces were much more evenly distributed and had lower magnitude (factor of 3.5 at the peak zone), for the composite cushion relative to the stiff seat. Moreover, the resonance frequency was lowered from a peak value of 4.5 Hz for the stiff seat to 2 Hz when a composite cushion was used.

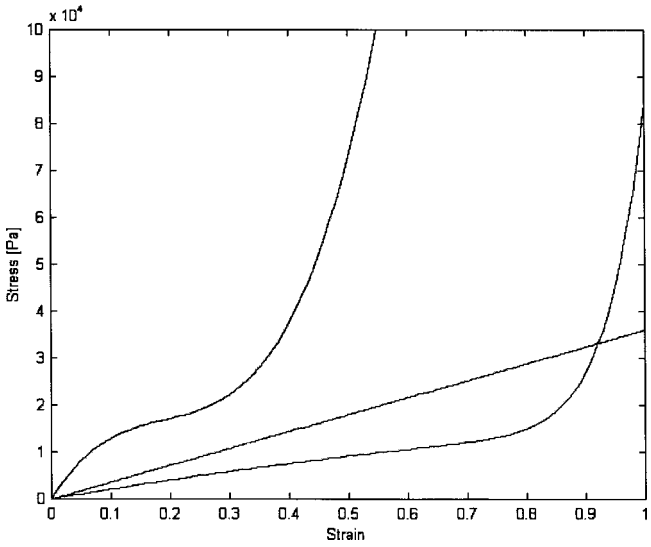

Fig. 7 Stress-Strain diagrams of the composite cushion component - experimental data

4 Conclusions

The main objective of this study was to develop a multi DOF lumped parameter model of the human body in a sitting posture, incorporating global dynamics in terms of apparent mass and local dynamics of the body/seat contact interaction. This model was further used for simulating different vibration axes, body posture, seat configuration, and input vibration magnitudes. Moreover, simulating the contact force distribution at the human/seat interface with various cushion configurations provided guidelines for designing cushions from the materials composition and structural/geometry perspective.

The parameters' optimization of the first subsystem of the multi DOF lumped parameter model, representing the apparent mass phenomenon of a seated human body, was based on the experimental database of Fairley and Griffin [8,9]. The experimental measurements of a seated human body apparent mass in the reference posture [8,9] suggested that the first mode of vibration appeared to arise from a motion of the whole upper body and the second mode of vibration arose from the horizontal response of the musculo-skeletal system, in which buttocks and the hips were out of phase with the shoulders. The model along the Z axis that was based on the 60 subjects database [8] simulated correctly the extended experimental data, with a resonance frequency at 4.25 Hz and a normalized apparent mass modulus factor of 1.5 with respect to the static mass on the sitting platform at the resonance frequency.

Experimental measurements with the backrest suggested that the seated body had only one mode of vibration. The effect of the backrest was particularly pronounced in the X direction [9]. As

seen in the experimental results, the major effect of the backrest was well expressed in the model by a significant increase of the viscoelastic parameter of the X direction relative to other vibration axes (Table 1). Moreover, the apparent mass modulus along the Z axis simulated by the model was smaller than the experimental results. This was done in order to maintain consistency with the findings of the reference posture. The model parameters were selected to preserve the same ratio between these two domains with and without the backrest.

The experimental results [8] showed that the greatest effect of the footrest position was at low frequencies, whereas minor effects were shown at frequencies above 10 Hz. For the footrest position in the range of 0–20 cm, the model simulations were in substantial agreement with the experimental results. However, the model was found to be limited in representing the experimental results in the frequency range of 0–1 Hz. A local minimum predicted by the model at that frequency range did not exist in the experimental data (for details, see [9]). Another limitation of the model was inability to represent the effect of the footrest in any position out of the 0–20 cm range.

The subjects exposed to vibration magnitudes in the range of 0.25–2 m/s^2 were using their lower back muscles to control the movement of the upper body [8]. The main phenomenon of decreasing human body stiffness to cope with increasing vibration magnitudes could be seen clearly in the second mode of vibration of the X and Y axes and in the first mode of the Z axis. Both the experimental and the model simulation results indicated that the stiffness of the musculo-skeletal structure is selective and nonlinear with respect to the input vibration magnitude.

The experimental data [8] and the model simulation indicated that the change in the resonance frequency caused by the muscle tension for an extreme range of voluntary muscle contraction levels was only 1.5 Hz. The experimental results indicated that the resonance peak became broader, and the value of the resonance increased as muscle contraction became more erect. The model simulated correctly the major effect of increasing both the resonance frequency and the apparent mass at the resonance frequency as the level of muscle contraction increased. However, the model failed to simulate the minor effect of the resonance peak that became wider as muscle tension increased. On the contrary, as the damping ratio of the upper body decreased, the resonance region became narrower.

Based on the model simulation and the extensive comparison to experimental databases, using a low number of DOF was found to be sufficient for simulating the major global apparent mass effect of a seated human body. One might claim that a more complex model is needed. However, the variability of body dynamics among the subjects examined experimentally [8,9] showed that the difference between the model and the experimental results is less than one standard deviation of the experimental results.

The second subsystem of the multi DOF model simulated the human pelvis and the target seat, from both geometrical and mechanical points of view, and predicted the vertical contact forces generated at the interface between them at the loaded strip. This strip was selected as the most significant two-dimensional signature of the three-dimensional human body/seat interface. For well defined vibration conditions (a frequency spectrum of 0–20 Hz with a magnitude of 1 m/s^2), the model simulation's results predicted the human body's main resonance frequency band and the dynamic contact force distribution both for static and dynamic conditions. Moreover, a very good correspondence between the experimental data [11,16], FEA [11,16,17] and the present lumped parameter modeling (LPM) approach was achieved in terms of the local peak generated by the Ischial Tuberosities (40–60 mm from the center line) and the general form of the stress distribution along the loaded strip (Fig. 8).

From the cushion design perspective, the best result among the materials and cushion geometry simulated in the current study in terms of evenly distributing contact forces was achieved by using a two-layer shaped geometry cushion built from three materials. The basic consideration for this development was the principle of uniform contact map. A composite cushion as a contact interface could cope with the unique anatomy of the human body exposed to a demanding vibration environment.

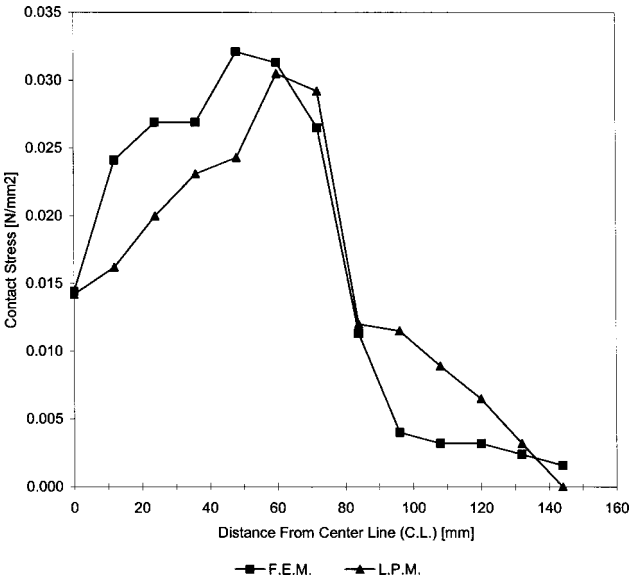

Fig. 8 Comparison of the static vertical contact stress distribution at the human body/composite flat cushion interface between lumped parameter model (LPM) and Finite Element Analysis/Model (FEA).

The immediate application of the model is as a design tool for developing human body protection devices. Whether the final product is a cushion, or a seat with a shock absorber, the ability to simulate the system using the human body's apparent mass model in various conditions may focus the development processes on the design procedure. The product's performance could be evaluated by using the model developed in this study to reduce the experimental work needed in the preliminary design stage.

Acknowledgment

Professor Mircea Arcan deceased on June 15, 2000. I thank him for lighting with his candle of wisdom my dark ways in the kingdom of knowledge.

References

[1] Corbridge, C., and Griffin, M. J., 1991, "Effects of Vertical Vibration on Passenger Activities: Writing and Drinking," Ergonomics, Oct. **34**(10), pp. 1313–1332.
[2] Griffin, M. J., and Brett, M. W., 1997, "Effects of Fore-and-aft, Lateral and Vertical Whole-body Vibration on a Head-positioning Task," Aviat Space Environ. Med., Dec. **68**(12), pp. 1115–1122
[3] Bovenzi, M., and Hulshof, C. T. J., 1998, "An Updated Review of Epidemiologic Studies on the Relationships Between Exposure to Whole-body Vibration and Low Back Pain," J. Sound Vib., **215**(4), pp. 595–611, August.
[4] Maskin, R., and Nash, C. D., 1976, "On Frequency Dependent Damping Coefficients in Lumped-parameter Models of Human Beings," J. Biomech., **9**, pp. 339–342.
[5] Patil, M. K., Palanichamy, M. S., and Ghista, D. N., 1978, "Man-tractor System Dynamics: Toward a Better Suspension System for Human Ride Comfort," J. Biomech., **11**, pp. 397–406.
[6] Nigam, S. P., and Malik, M., 1978, "A Study on Vibratory Model of a Human Body," J. Biomed. Eng., **109**, pp. 148–153.
[7] Amirouche, F. M. L., and Ider, S. K., 1988, "Simulation and Analysis of a Biodynamic Human Model Subjected to Low Acceleration—a Correlation Study," J. Sound Vib., **123**(2), pp. 281–292.
[8] Fairley, T. E., and Griffin, M. J., 1989, "The Apparent Mass of the Seated Human Body: Vertical Vibration," J. Biomech., **22**(2), pp. 81–94.
[9] Fairley, T. E., and Griffin, M. J., 1990, "The Apparent Mass of the Seated Human Body in the For-and-aft and Lateral Directions," J. Sound Vib., **139**(2), pp. 299–306.

[10] Arcan, M., and Brull, M. A., 1980, ''An Experimental Approach to the Contact Problem Between Flexible and Rigid Bodies,'' Mech. Res. Commun., **7**(3), pp. 151–157.
[11] Brosh T., 1990, ''Mechanical Parameters Characterizing Basic Sitting Posture—A Contact Mechanics Approach,'' Ph.D. Thesis, Tel-Aviv University.
[12] Brienza, D. M., Chung, K.-C., Brubaker, C. E., Wang, J., Karg, P. E., and Lin, C. T., 1996, ''A System for the Analysis of Seat Support Surfaces Using Surface Shape Control and Simultaneous Measurement of Applied Pressures,'' IEEE Trans. Rehabil. Eng., **4**(2), pp. 103–113.
[13] Prutchi, D., and Arcan, M., 1993, ''Dynamic Contact Stress Analysis Using a Compliant Sensor Array,'' Measurement-Journal of the International Measurement Confederation, **11**, pp. 197–210.
[14] Sprigle, S. H., Chung, K. C., and Brubaker, C. E., 1990, ''Reduction of Sitting Pressures with Custom Contoured Cushions,'' J. Rehabil. Res. Dev., **27**(2), pp. 135–140.
[15] Brienza, D. M., Lin, C. T., and Karg, T. E., 1999, ''A Method for Custom-Contoured Cushion Design Using Interface Pressure Measurements,'' IEEE Trans. Rehabil. Eng., **7**(1), pp. 99–108.
[16] Brosh, T., and Arcan, M., 2000, ''Modeling the Body/chair Interaction—An Integrative Experimental-Numerical Approach,'' Clin. Biomech. (Los Angel. Calif.), **15**(3), pp. 217–219.
[17] Comisioneru, S., 1991, ''Body/cushion Contact Stress Analysis During Sitting,'' M.Sc. Thesis, Tel-Aviv University.
[18] Fung, Y. C., 1993, *Biomechanics—Mechanical Properties of Living Tissue*, Springer Verlag.
[19] Mow, V. C., and Hayes, W. C., 1991, *Basic Orthopedic Biomechanics*, Raven Press.
[20] Harris, C. M., and Crede, C. E., 1976, *Shock and Vibration Handbook*, 2 edition, McGraw-Hill.